UNIVERSITY OF OKLAHOMA

GRADUATE COLLEGE

MANUFACTURING OF CARBON NANOTUBE-EPOXY COMPOSITES AND TESTING OF THE PHYSICAL AND ELECTRICAL PROPERTIES

A THESIS

SUBMITTED TO THE GRADUATE FACULTY

In partial fulfillment of the requirements for the

Degree of

MASTER OF SCIENCE

By

Dongfang 'Steven' Zhao

Norman, Oklahoma

2024

MANUFACTURING OF CARBON NANOTUBE-EPOXY COMPOSITES AND

TESTING OF THE PHYSICAL AND ELECTRICAL PROPERTIES

A THESIS APPROVED FOR THE

SCHOOL OF AEROSPACE AND MECHANICAL ENGINEERING

BY THE COMMITTEE CONSISTING OF

Dr. Yingtao Liu, Chair

Dr. Hanping Ding

Dr. Christopher Billings

Acknowledgment

First, I want to express my gratitude and appreciation to my advisor and mentor Dr. Yingtao Liu. His dedication, continuous support, and patience enabled the SMIS lab, his students, and me to pursue our goal and find our place in the academic world. Dr. Liu took me under his wing when I was still a junior in undergraduate school, and I have been studying and researching under his guidance ever since. I cannot thank Dr. Liu enough for his effort, patience, and trust in my last five years at OU.

Next, I would like to thank Dr. Kurt Gramoll, Dr. David Baldwin, Dr. Wilson Merchán-Merchán, and again Dr. Liu, for their teaching and knowledge during my undergraduate studies, where I built a strong foundation of my engineering and research skills. Then, I want to thank Dr. Kuang-Hua Chang, Dr. Jivtesh Garg, Dr. Mrinal Saha, and Dr. M. Cengiz Altan for their support and teaching in my graduate study years. Their expertise in the field helped me navigate my research and projects. I would also like to thank Dr. Hanping Ding and Christopher Billings for being on my thesis committee and contributing their precious time and expertise in the field.

The AME office has been a tremendous help during my years in OU, in the Department of Aerospace and Mechanical Engineering. Among the faculty and staff members, Dr. Ramkumar Parthasarathy was particularly helpful to me. He helped me with all kinds of paperwork that I had to do, with my TA opportunities, and advice on internships.

I would also like to thank the AME machine shop for their support during all my research and projects during my time here at OU, especially Bill Mays, Greg Williams, and Elijah Personette. Without their help, a lot of my designs and ideas would not have become reality.

During my time here in the SMIS lab, I have had a lot of help and inspiration from colleagues and friends, I want to mention their names: Blake Herren, Christopher Billings, Peter Sandell, Benjamin Sherwood, Jacob Meves, Lane Tayler, Cameron Collum, Anirban Mondal, and Ian Kennedy. Out of all my colleagues, Blake Herren and Christopher Billings joined the SMIS lab long before me, and it was their help and insights that got me through the beginning of my time in the lab when I barely knew anything about 3D printing and composite materials.

At Last, I just want to say that I would not have been able to achieve this without the support of my family. It has been tough for both me and my family, living across the ocean, and only able to see each other through electronics, but they encourage me to keep pushing forward and pursue my future.

Table of Contents

List of Figures

List of Tables

Abstract

The development of multi-functional smart materials has been rapid in the materials community in recent years. Shape memory nanocomposite material has been studied extensively. In this research, the epoxy resin-based shape memory composite material mixed with a multi-walled carbon nanotube (MWCNT) can change shape when stimulated by heat. Different designs of the printed nanocomposites and their ability to change shape without damaging themselves are explored. In addition, due to the presence of MWCNTs, the developed nanocomposite is electrically conductive and can be used as a strain and deformation sensor due to its piezoresistive sensing capability. The developed nanocomposite sensors are studied as embedded sensors for structural health monitoring (SHM) [1, 2], which is essential for providing real-time assessments of composite structures, enhancing safety, and extending their service life. Early damage detection through advanced nanocomposite sensors enables timely maintenance, reduces costs, and helps prevent catastrophic failures. This thesis introduces the synthesis, 3D printing, and characterization of novel embedded strain sensors using MWCNT-enhanced nanocomposites in fiberglass-reinforced composites for potential damage diagnostics and SHM applications. MWCNTs are dispersed within the structural epoxy to create 3D-printed nanocomposites with piezoresistive sensing capabilities. These sensors are embedded in fiberglass-reinforced composite laminates, and their performance is characterized under various maximum loads and load rates during three-point bending tests. Additionally, the long-term reliability of the strain sensors is evaluated over 1000 loading cycles. The recorded piezoresistive signals demonstrate high sensitivity to applied bending loads, with a gauge factor of up to 100, indicating strong potential for load sensing, in-situ damage diagnostics, and real-time SHM in structural composites.

1. Introduction

Polymer nanocomposites are materials that combine polymers (large, chain-like molecules) with nanofillers (extremely small particles, typically in the range of 1-100 nanometers) [3]. Including these nanoparticles can significantly enhance the properties of the base polymer, leading to a material with superior characteristics compared to traditional polymer composites.

Polymers are long, repeating chains of molecules, known for their versatility and wide range of applications. Common polymers used in nanocomposites include polyethylene, polypropylene, polystyrene, epoxy resins, and polyesters. When we refer to nanomaterials, we refer to materials with at least one dimension in the nanometer scale. Common types of nanomaterials used in polymer composites include nanofibers, nanoclays, graphene, and carbon nanotubes (CNTs). This research is focused on all aspects of the composition of epoxy resin and CNTs, which includes the raw materials, manufacturing process, properties, applications, challenges, and future.

Epoxy resin is a versatile and widely used thermosetting polymer (solidifies under high temperatures), known for its strong adhesive properties, chemical resistance, and excellent mechanical properties. It is a key material in various industrial, commercial, and DIY applications, often as a structural matrix, adhesive, coating, or composite material. Epoxy resin typically consists of two main components: the epoxy, and the curing agent (hardener). Without the hardeners, sole epoxy resin will have a hard time solidifying and curing, achieving the desired results. Epoxy resin is usually a clear or slightly colored viscous liquid. The most common type of epoxy resin is derived from a reaction between epichlorohydrin and bisphenol-A (BPA), resulting in a compound known as diglycidyl ether of bisphenol-A (DGEBA) [4]. When epoxy resin is mixed with hardeners, a process called polymerization will be initiated, forming a cross-linked polymer network. It is generally used in applications such as adhesives, coating, electronics, etc.

The epoxy used in this research is called Epon-862 (diglycidyl ether of bisphenol F), an engineering-grade resin designed for crafting, construction, and lab research. It has many benefits such as low viscosity, low color, good chemical resistance, and can react to a wide range of hardeners. [5]. The hardeners, or curing agents, used in this research are Epikure 9553 and Epikure W. This unique combination of epoxy resin and hardeners gave the product shape memory ability, enabling geometry manipulation when it reaches its glass transition temperature [6].

Multiwalled carbonnanotubes (MWCNTs) are a type of carbon nanotube (CNT), which are cylindrical nanostructures composed of rolled-up sheets of graphene (a single layer of carbon atoms arranged in a hexagonal lattice). Unlike single-walled carbon nanotubes (SWCNTs) which consist of a single graphene cylinder, MWCNTs, as the name suggests, are made up of multiple layers of rolled-up graphene sheets. Therefore, MWCNTs have a larger diameter than their single-walled counterparts, plus it is easier and cheaper to make. The outer diameter of MWCNTs is usually 1-100 nm, the particular ones used in this research are around 50 nm.

Because the carbon element is conductive, MWCNTs are excellent electrical conductors, making them useful in applications that require high conductivity, such as in conductive films, cables, sensors, and electrodes. MWCNTs also exhibit exceptional tensile strength, which can massively increase the mechanical characteristics of the product when mixed with a matrix. This makes them ideal for reinforcing materials in composites. In this experiment, the base material Epon 862 is mixed with a set percentage of MWCNTs with respect to weight.

Polymer nanocomposites have great mechanical properties such as high strength, toughness, stiffness, and strength-to-weight ratio [7, 8] and also possess excellent barrier properties [9]. Due to the dense structure of the crosslinked polymer, they are more resistant to corrosion and erosion from gases, moisture, and chemicals than most other metals, alloys, or plastic.

Though there are many advantages of polymer composites over traditional materials, many challenges still stand in the way of the desired outcome of this product, such as nanoparticle filler dispersion. Achieving a uniform distribution of nanoparticles is key to maximizing their effectiveness. Aligned nanofibers can significantly increase the composite's strength, whereas misaligned or poorly dispersed nanofibers can cause agglomeration [10]. Good bonding between the matrix and fiber is also critical for the structural integrity of the composite. With poor adhesion between the fiber and the matrix, many types of failures, such as fiber pullout, fiber breakage, delamination, matrix cracking, etc., can happen to the product [11]. The materials can also be expensive, from engineering-grade epoxy resin to CNTs, where each jug of materials could easily cost hundreds of dollars. And not to mention the waste of materials in the lab because the manufacturing process is not industrialized and streamlined. Lastly, the potential for chemical hazards should not be overlooked, as many ingredients harm human health.

Additive manufacturing (AM), commonly referred to as 3D printing, has become a powerful technique for fabricating embedded sensors within composite materials. AM technologies offer precise control over the fabrication process, enabling the integration of intricate sensors with high spatial resolution directly into composites. Various polymer-based AM methods, such as fused deposition modeling (FDM), stereolithography (SLA), digital light processing (DLP), and direct ink writing (DIW), have been employed for in-situ manufacturing of embedded sensors in structural composites.

FDM-based polymer AM is widely accepted for 3D printing thermoplastic nanocomposites with self-sensing capabilities. SLA and DLP technologies are wellregarded for achieving high surface smoothness and geometric accuracy, making them ideal for printing load sensors. The AM method discussed in this research, DIW-based polymer AM, offers unmatched versatility in material selection, accommodating conductive polymers, metallic inks, and nanocomposite inks to customize embedded sensors' electrical and mechanical properties [12, 13]. Furthermore, the precision and control offered by the DIW process enable multi-material 3D printing, facilitating the creation of advanced, multifunctional sensors with layered or gradient functionalities [14] as we mentioned before, which excels in the fabrication of embedded strain sensors. While the benefits of the DIW method in polymer nanocomposite fabrication are clear, the problems and disadvantages of this method have also come to researchers' attention. One of the biggest challenges in this field is achieving good nanoparticle alignment. Because the ink is dispensed through a small nozzle, DIW processes often struggle to control the orientation of nanomaterials within the printed layers, limiting the full exploitation of their potential. The resolution and precision of the prints can also be limited by the performance of the 3D printer and other hardware, sometimes giving inconsistent results. The fabrication speed is also another factor in the way of upscaling the manufacturing process, slowing down the fabrication speed and research progress. Last but not least, many additive-manufactured nanocomposites require pre and post-processing, such as degassing [15], polishing, autoclave curing [16], etc.

The DIW printer used in this research is converted from a traditional FDM printer, with both software and hardware modified to fit the needs. Due to the highly customizable nature of a modified DIW printer, many detailed printing parameters were further explored in this experiment, such as nozzle travel speed, dispense nozzle size (diameter), layer height, extrusion pressure, print patterns, etc.

This research focuses not only on the shape memory capability of the material but also the polymer composites' electrical conductivity and their potential for sensory, as they are manufactured into embedded strain sensors. Due to the flexibility of the epoxy-MWCNT composite, they have a large elastic region and can withstand more deformation than traditional materials. This feature inspired its application in structural health monitoring and damage diagnostics [17], which can be applied to many industries such as aerospace, automobile, construction, etc.

Embedded sensors and networks enable certain structural composites to monitor their health and provide real-time feedback on structural integrity. This self-sensing capability extends the lifespan of composites and enhances the safety of entire composite structures and systems. Such innovations can significantly reduce maintenance costs, minimize downtime, and prolong the service life of composite structures. The integration of advanced sensors and sensing networks for damage detection has led to the development of complex structural health monitoring (SHM), damage diagnostics, and prognostics over the past two decades.

Many other researchers in the field have taken similar approaches to fabricating sensor devices with polymer nanocomposites [18-20]. Das et al. have presented the potential applications of many polymer nanocomposite sensors such as strain sensors, electrochemical sensors, biosensors like glucose and cholesterol sensors, gas and humidity sensors, and organic vapor sensors [21]. There are even self-healing sensors made of chitosan (CS) and MWCNT, that can repair themselves with the assistance of water vapor [22, 23]. Some sensors can even detect delamination within the composite [24].

This thesis intends to discuss the current work done on this unique shape memory epoxy, and possible plans and improvements. The next section will discuss the nanocomposite's raw materials and manufacturing process. After that, 3D printing parameters will be explored as one of the main focuses of the study. The samples' Mechanical and electronic properties will also be tested and evaluated in detail. Finally, discussions will be conducted on this study, from its manufacturing to the properties of the final product. The advantages and disadvantages of this method will be explored, and finally, the uniqueness of the findings will be discussed.

2. Manufacturing

2.1. Materials

All the raw materials used during this research is used as received, without modification. The epoxy resin Epon 862 (diglycidyl ether of bisphenol F), along with the two curing agents Epikure 9553 and Epikure W, were all purchased from Hexion. The MWCNT used in the research was purchased from Sigma Aldrich, it has a diameter of 50-90 nanometers and an aspect ratio of 100. The Fiberglass tape used for the embedded sensor has a width of 1 inch, and it is purchased from Fiberglast. Lastly, the 3D printer used in the research is a modified Creality Ender 3 FDM printer turned into a DIW printer with custom-made extruders.

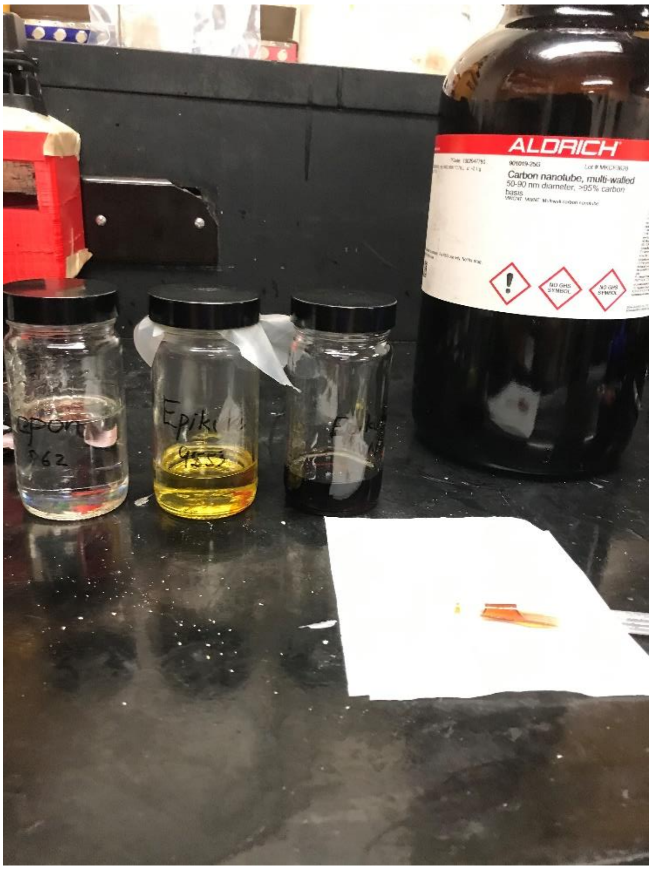

Figure 1. Raw Materials for the Composite

2.2. Preparation and Manufacturing

A 1.5 wt.% concentration of multi-walled carbon nanotubes (MWCNTs) was dispersed in Epon 862 epoxy resin to prepare a nanocomposite suitable for 3D printing using a direct ink writing (DIW) process. The MWCNTs were uniformly dispersed in the epoxy resin by mixing them for 10 minutes in a planetary Thinky AR100 mixer. Next, two curing agents were hand-mixed for two minutes in a 1:1 molecular ratio and then added to the MWCNT/epoxy mixture. This combined mixture was further processed in the Thinky AR100 mixer for five minutes to ensure complete integration of the nanoparticles and resin.

After mixing, the nanocomposite was transferred to a syringe and placed in a centrifuge for additional mixing and degassing for over five minutes. Theoretically, the longer the mixing/degassing time the better the product will turn out, with better CNT dispersion and less porous structures within, but since this composite has the properties of thermal set plastics, mixing for an extended period in the mixer will generate heat and increase the viscosity, making it harder to extrude from the nozzle. The degassed nanocomposite was loaded into a 10-cc syringe and mounted onto a custom pneumatic-driven DIW printer, which had been modified to accommodate the nanocomposite material. The manufacturing process resulted in a black goo-looking paste, and a 25-gauge dispensing nozzle was used for precise deposition during printing. When extruded and cured, it will become a nanocomposite with shape memory capability and conductive.

To test its sensing capability as an embedded sensor, the nanocomposite will be enclosed by fiberglass fabrics. A fiberglass fabric tape (6 inches long and 1 inch wide) was secured onto the build plate of the DIW 3D printer, and the nanocomposite was printed directly onto the center of the tape under a constant pressure of 20 psi. After printing, two copper wires were embedded into the electrodes at each end of the strain sensor, and the setup was left to solidify overnight at room temperature.

For the wet layup process of composite laminates without MWCNTs, pristine Epon 862 resin and the same curing agents were mixed. The 3D-printed nanocomposite strain sensor and five additional layers of fiberglass fabric were stacked using the wet layup technique. The 3D-printed sensor was embedded within the composite laminate and covered by one layer of fiberglass fabric, creating embedded sensors within the composite samples. The final composite laminates were pressurized using a vacuum bagging process at room temperature for eight hours, followed by post-curing at 180°C for two hours. The final thickness of the composite was 2.2 mm ± 0.2 mm. Figure 2 offers a visualization of the process. Once completed, the samples will be tested to characterize their mechanical properties and piezoresistive sensing capabilities.

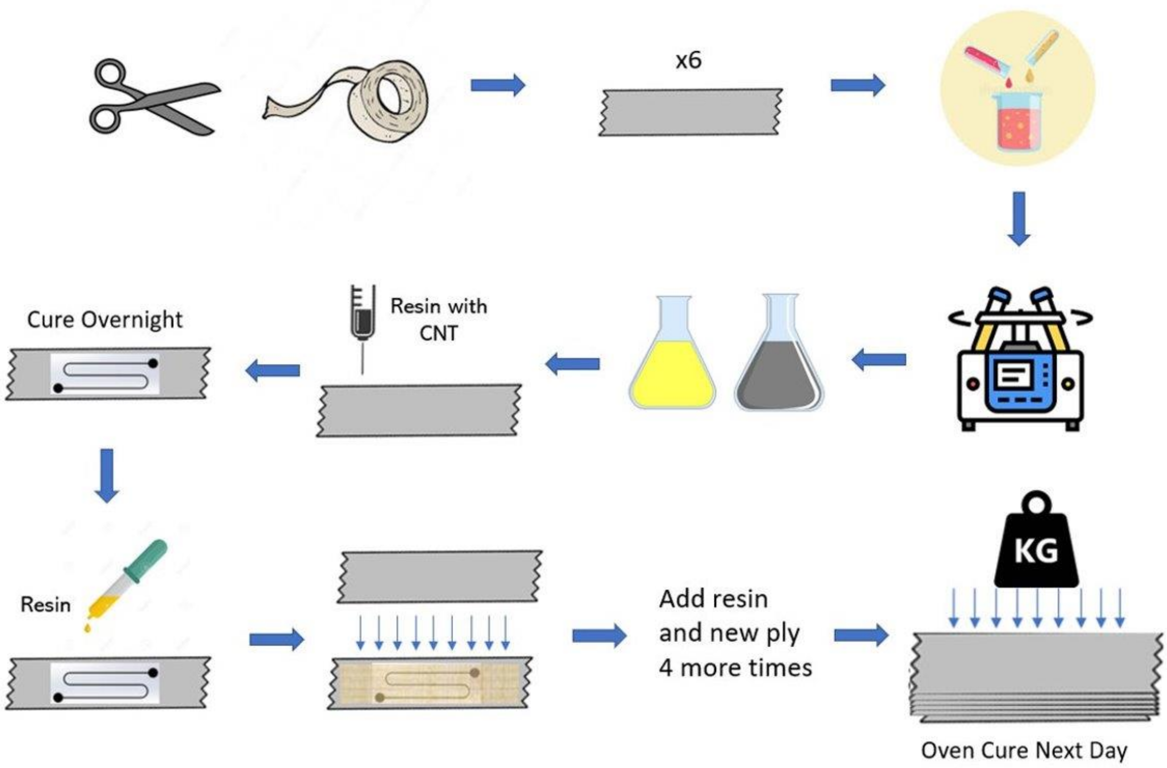

Figure 2. Material Preparation and Manufacturing Process

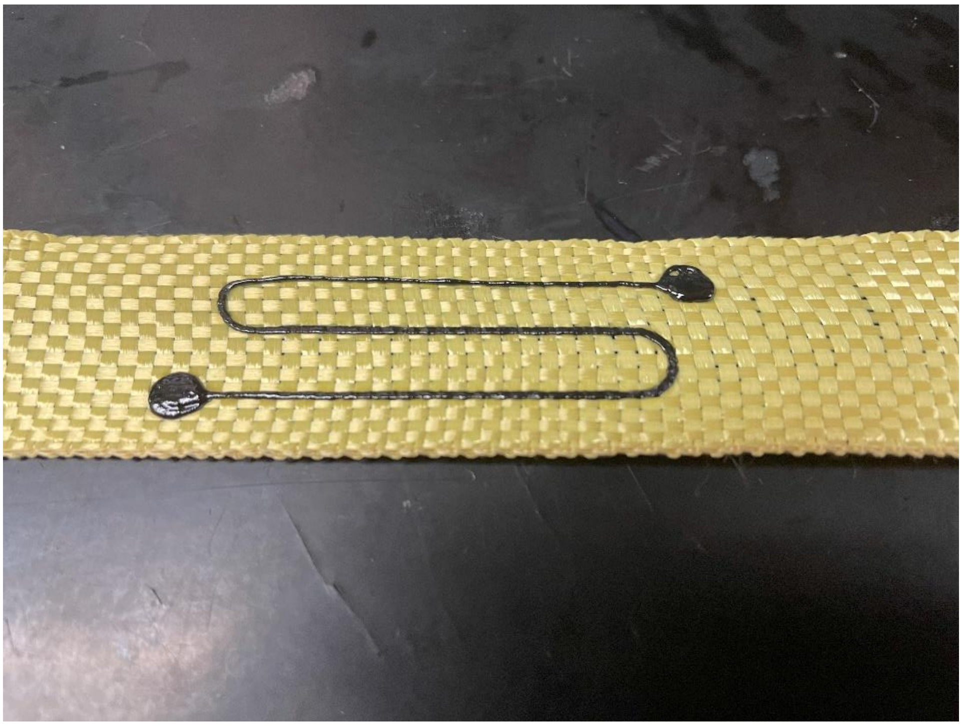

Figure 3. Line Print Acting as Sensor on Fiberglass Tape

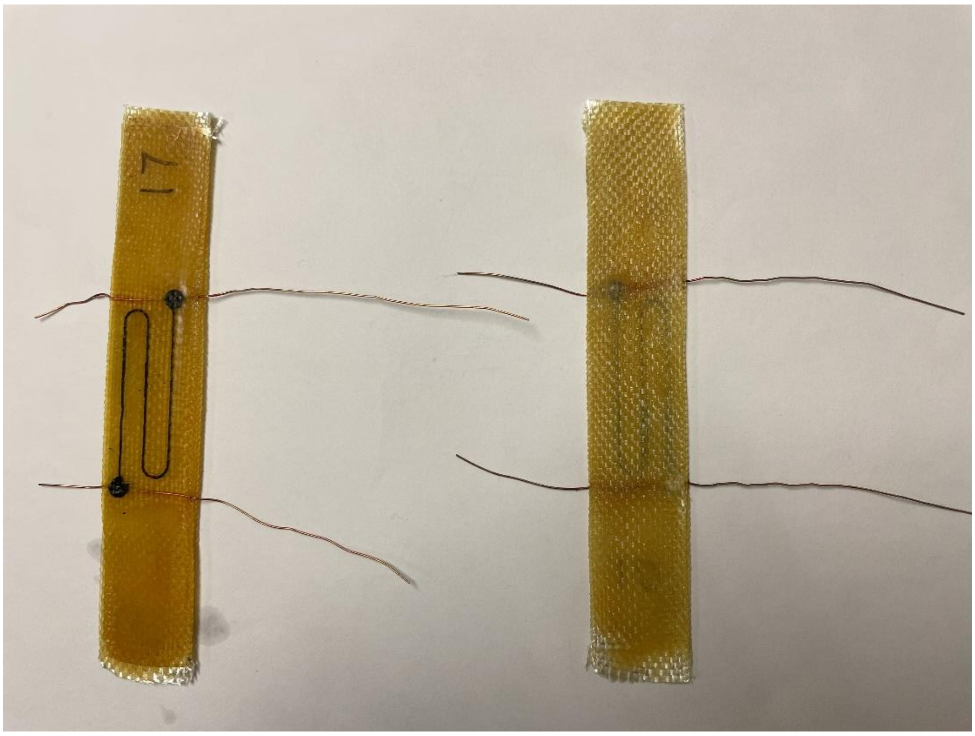

Figure 4. Completed Embedded Sensor

3. 3D Printing with Prepared Composite

3.1. Printing Setup

A Direct Ink Writing (DIW) printer fabricates the nanocomposite in this experiment. Direct Ink Writing (DIW) is an additive manufacturing (AM) technique used to print highly viscous inks and pastes, allowing the fabrication of complex 3D structures with precise material placement. Unlike other AM technologies that rely on melting or curing solid materials, DIW extrudes materials directly in a fluid or paste-like form, solidifying after deposition. It is highly versatile and capable of printing various materials with rheology that is difficult to print with other printing methods [25], including polymers, nanocomposites, hydrogels, ceramics, and even biomaterials. With more modification, it can even achieve multi-material extrusion by adding more extruders and cartridge feeds, along with software configurations. DIW printing is one of, if not the most common methods for nanocomposite printing, printed materials are often used as sensors, electrodes, circuits, medical implants, and many others. With all the benefits of DIW printing, one of the biggest challenges it faces is the pre-processing and post-processing of printing material. The printed material must be kept at a good balance between viscosity and flowability, and printed materials often require additional curing or sintering to achieve the desired result. Due to many restraints, DIW-printed materials often fail in mechanical strength in comparison to traditionally manufactured materials.

This specific printer used in the experiment is a modified Creality Ender 3 printer as shown below. The original printer is an FDM printer with a heated extruder nozzle and a heat bed. To convert it into a DIW printer, the two components mentioned earlier will have to be replaced by pneumatic-powered DIW printer parts.

Figure 5. Unmodified Ender 3 FDM printer

First, the heated plastic extruder is taken out completely, along with the cartridge rack and feed tube. A custom-made syringe holder has taken the place of the extruder, and a pressure regulator is fixated on the top left corner of the frame, held by a 3D-printed scaffolding. The inlet of the pressure regulator is connected to the compressed air source through a rubber tubing and can be turned on and off by a valve on the wall (Figure 4).

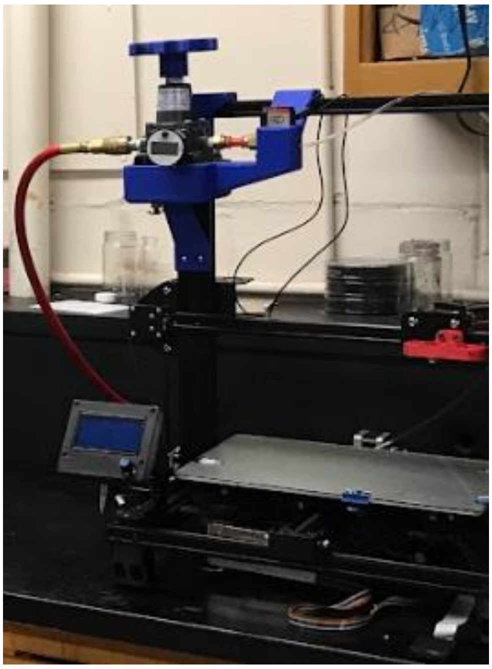

Figure 6. Pressure Regulator and Syringe Holder

The pressure regulator outlet is connected to thinner rubber tubing with a specially made air-tight connector designed to lock onto 3cc and 10cc syringe tubes (see Figure 5). This setup allows constant air pressure to be pumped into the syringe containing the ink and extruded through the dispensing nozzle of different diameters. The valve on the pressure regulator allows manual pressure to change during the printing process.

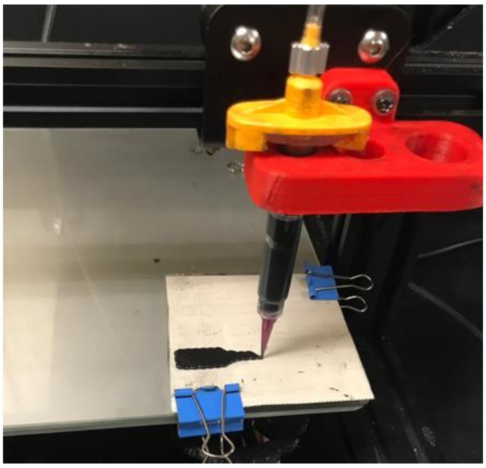

Figure 7. Air-Tight Syringe Connector

The heat bed from the FDM printer was also replaced with a regular glass panel, as the nanocomposite ink does not need to be heated during any part of the printing process, and glass is easier to clean after print jobs.

Hardware aside, the printer's software has also been altered to compensate for the new modules. The temperature controls on the extruder head and bed have been disabled since they are no longer needed. The cooling fan control on the original extruder head has been modified to control the new pressure regulator, essentially acting as a switch for the airflow. The X, Y, and Z axis motor function is kept the same. The slicing software used to create Gcode on this printer is Repetier Host, a common and handy slicer for most types of printers. It takes the .stl format of the CAD file created from software such as Solidworks and AutoCAD and turns them into a large file of Gcode that can be understood by the printer. After creating the Gcode, it will be moved and stored in a micro-SD card from the computer and inserted into the printer.

3.2. Printing Parameters

When using a DIW printer, various printing parameters play a crucial role in determining the quality, precision, and performance of the printed part. These parameters need to be carefully optimized depending on the type of ink, material formulation, and desired output.

Ink viscosity is one of the most important factors for DIW printing, as it affects the flowability and the ease of extrusion through the nozzle. The ink must be viscous enough to retain its shape after deposition but fluid enough to flow smoothly through the nozzle. The proper viscosity is discovered through trial and error while mixing the raw materials.

Extrusion pressure controls the flow rate of the material. Higher pressures are needed for more viscous inks, while lower pressures are used for less viscous materials. Too much pressure can lead to over-extrusion, while too little may result in under-extrusion. In this experiment, a constant pressure of 20 to 30 psi was used during print. However, the pressure needed to be turned up towards the end of bigger prints, and this introduced another factor called pot life [26]. Pot life is a measurement of time in composite materials, especially the ones already mixed with curing agents. The pot life indicates the time it takes for the epoxy or the base material to solidify to the point where it reaches a very high viscosity and cannot be extruded, often after mixing with curing agents. For this epoxy resin-MWCNT composite used in this experiment, the pot life is around 40 minutes to 1 hour after it is loaded into the syringe and mounted on the printer. Toward the end of the pot life, the material often becomes more difficult to extrude under the current 20 psi air pressure, and the regulator valve needs to be turned up to increase the air pressure, thus ensuring successful prints without breakage of ink.

The internal diameter of the dispensing nozzle is also important for the quality of the prints. The nozzle diameter directly affects the resolution and thickness of the printed lines or layers. Smaller nozzles provide finer detail but may require higher pressures to extrude viscous materials. After trying out nozzles with different diameters, a 25-gauge nozzle is selected that best matches the current printing pressure, layer height, and nozzle travel speed. In the medical dispenser conversion chart, 25 gauge is the equivalent of 0.01 inch or 0.25 mm. The diameter of the nozzle also represented the layer height of the print, as the ink coming out from the nozzle is in a cylindrical shape.

Figure 8. Dispense Tips of Different Sizes [27]

Print speed influences layer quality, adhesion, and accuracy. Slower speeds allow for more precise deposition and better material adhesion, while faster speeds reduce printing time but can compromise accuracy and layer bonding. The print speed of 5 mm/s is used for the dog bone samples and other complex shapes for shape memory testing and demonstration, whereas the print speed of 10 mm/s is used for printing a single line as the embedded sensor.

The printing pattern will not only determine the structure of the print but also affect its mechanical properties. Certain patterns, like zigzag, honeycomb, or concentric circles, may enhance material bonding or reduce material usage. A rectilinear pattern was first used to make dog bone samples, where the print path runs diagonally to the length of the specimen. However, this pattern was quickly abandoned because the focus of the experiment at the time was to test the tensile strength of the specimen. After some adjustments, a new pattern is adopted and the print path travels parallel to the length of the specimen, giving it maximum potential in a tensile strength test.

Figure 9. Rectilinear (left) and Straight-Line (right) Samples

Like many DIW materials, this epoxy-based nanocomposite also requires post-print curing to achieve its full functionality. Based on the information given by the distributor of the epoxy, the printed specimen should stay and naturally cure in a room-temperature environment overnight, and cure in a 180 degrees Celsius oven for two hours the next day.

4. 3D Printing of Various Shapes and Shape Memory Ability

Besides the ASTM D790 dog bone shape, many different shapes were printed for testing and demonstrating the material's shape memory ability. This special combination of Epon 862 with Epikure 9553 and Epikure W gives the composite the ability to change shape when temperature changes. The material has a glass transition temperature [28] of 120 degrees Celsius. When it reaches that temperature, the material is no longer stiff like a solid, it becomes rubbery, and its shape can be physically manipulated without breaking.

The first shape printed is an imitation of a flower, with five petals connected in the middle. The aim is to fold the petals while the materials are over their glass transition temperature, then unfold with the help of some outside heat source.

Figure 10. Flower Shaped Print

To get the material over its glass transition temperature, a Petri dish of cooking oil is placed on a hot plate, and once the desired temperature has been reached, the specimen will be submerged in the oil bath. A pair of tweezers were used to handle and manipulate the shape of the specimen.

Figure 11. Specimen Submerged in Oil Bath

Once the specimen's shape has changed, it is allowed to cool down and it will stay in the new shape unless heated up to the glass transition temperature again. The pictures below demonstrate how the specimen returned to its original shape when heated.

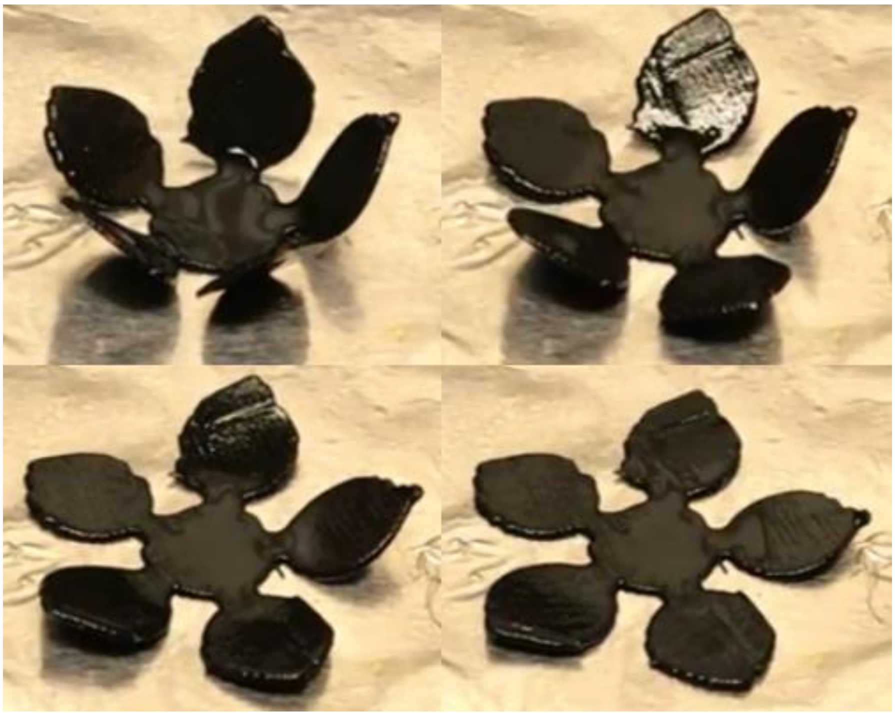

Figure 12. Flower Print Returns to Its Original Shape

Many other shapes were also printed and tested similarly, as shown below.

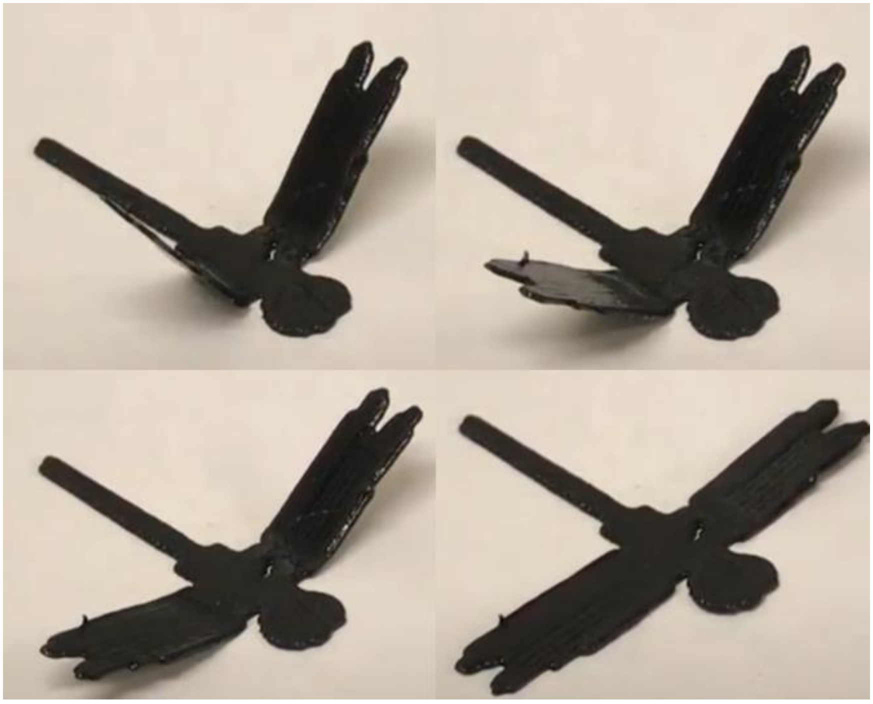

Figure 13. Dragonfly Imitation

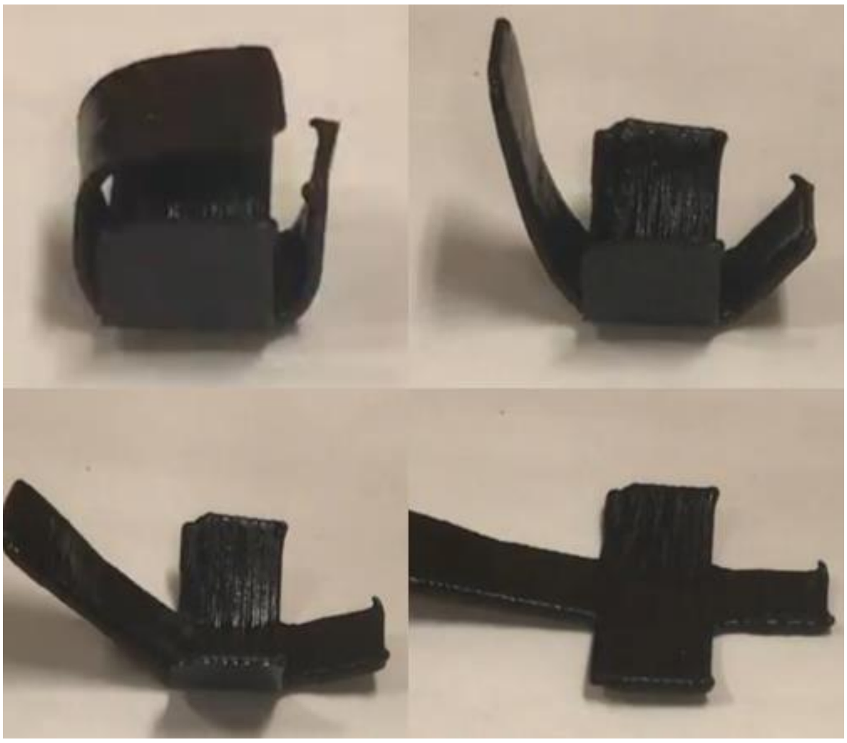

Figure 14. Cube Imitation

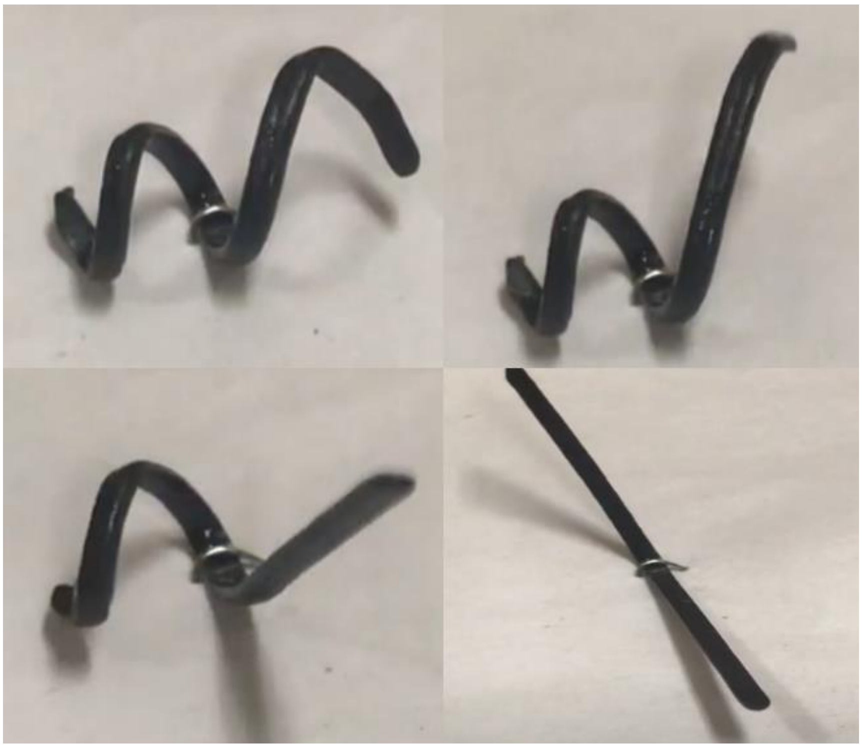

Figure 15. Spiral Returns to Line

The material demonstrated that it could memorize shape with the help of an external heat source, and this cycle can be repeated many times without degradation and damage. The unique feature of this material could lead to the possibility of 4D printing [29, 30], where heat and shape change play a big role.

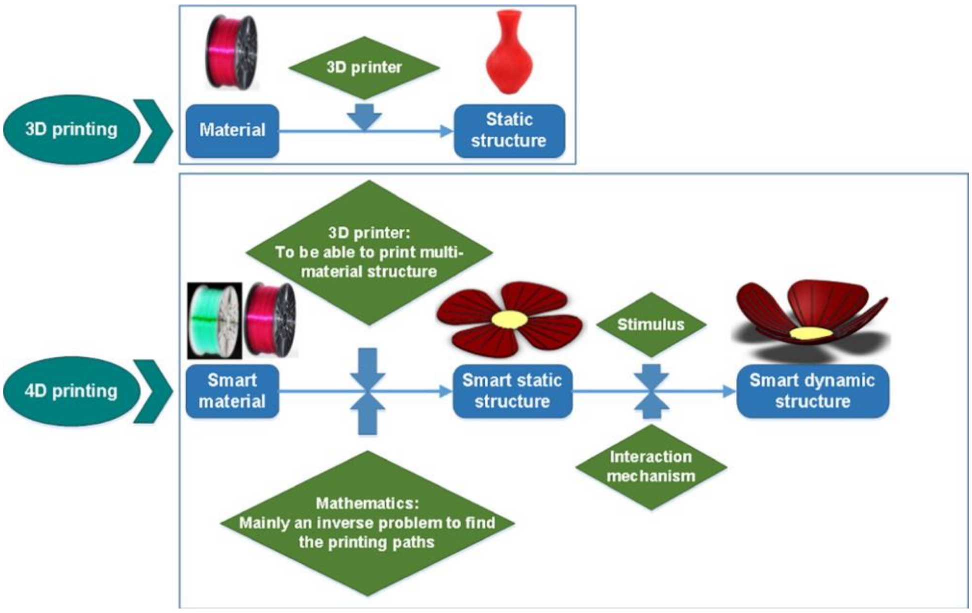

Figure 16. Difference between 3D Printing and 4D printing

To achieve 4D printing, a lot more modifications would have to be made to the printer, and possibly integrate the printer with the oven to provide heat stimulation. This is potentially a huge project and would most likely be a project for the future.

5. Electrical Properties and Analysis

Line-shaped sensors embedded in layers of fiberglass tape are prepared to test the electrical conductivity of the nanocomposite and its ability to perform as piezoresistive sensors. To make these embedded sensors, An Instron 5969 mechanical testing system was utilized for the characterization of the piezoresistive sensing capability of the 3D printed and embedded strain sensors in composite laminates under 3-point bending load, following the ASTM D790 standard. The flexural strain was calculated using the experimental data recorded by the Instron system following the equation below:

$$\varepsilon_f = 6Dd/L^2$$

where ε_f is the flexural strain, D is the maximum deflection of the center of the beam, L is the support span length, and d is the thickness of the composite sample.

A HIOKI resistance meter was connected to the copper wires that extended out of the composite sample to record the change in resistance during the test. The piezoresistive sensing singles were continuously recorded during the entire mechanical test. To determine the appropriate load range, a sample was first tested until failure to determine the maximum applicable load, which was identified to be 210 N. Since the long-term sensor performance should be fully understood in this study, we decided to choose the maximum load of 35N, 70N, 105N, and 140N for cyclic tests and sensor characterization. Additionally, different strain rates were also employed to fully understand the effect of the applied strain rate on the piezoresistive sensing performance. Moreover, we studied the long-term sensor performance under cyclic loading conditions up to fatigue 1,000 cycles. Figure 2b shows the experimental setup of the 3-point bending using the Instron system and the HIOKI resistance meter.

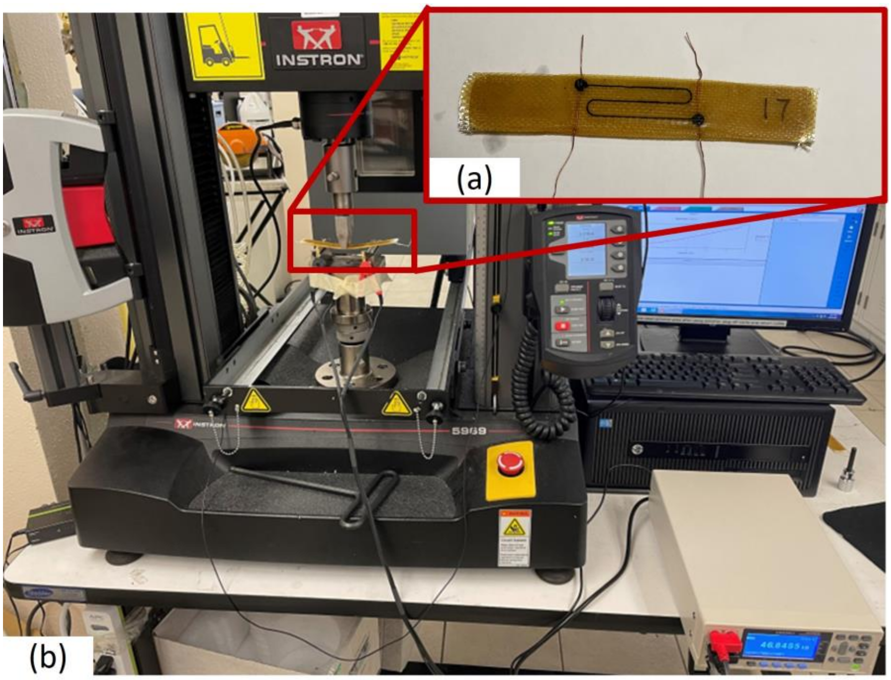

Figure 17. (a) Manufactured fiberglass reinforced composites with embedded MWCNT and epoxy nanocomposites as strain sensors for load sensing and damage detection; (b) Experimental setup of piezoresistive sensor testing under 3-point bending

The performance of the 3D printed and embedded strain sensors was first characterized under quasi-static loads. Composite beam samples were tested under 3-point bending loads at the load rate of 10 mm/min and up to four maximum applied loads of 35 N, 70 N, 105 N, and 140 N, respectively. Figure 18a illustrates the piezoresistive sensing responses under these specified loads. Notably, all measured signals exhibited both a high signal-to-noise ratio and consistent repeatability. At the lower end, a maximum load of 35 N yielded minimal strain, leading to subdued piezoresistive sensing outputs. However, as the applied load intensified, there was a corresponding amplification in the sensor signals. The applied loads are shown in Figure 18b.

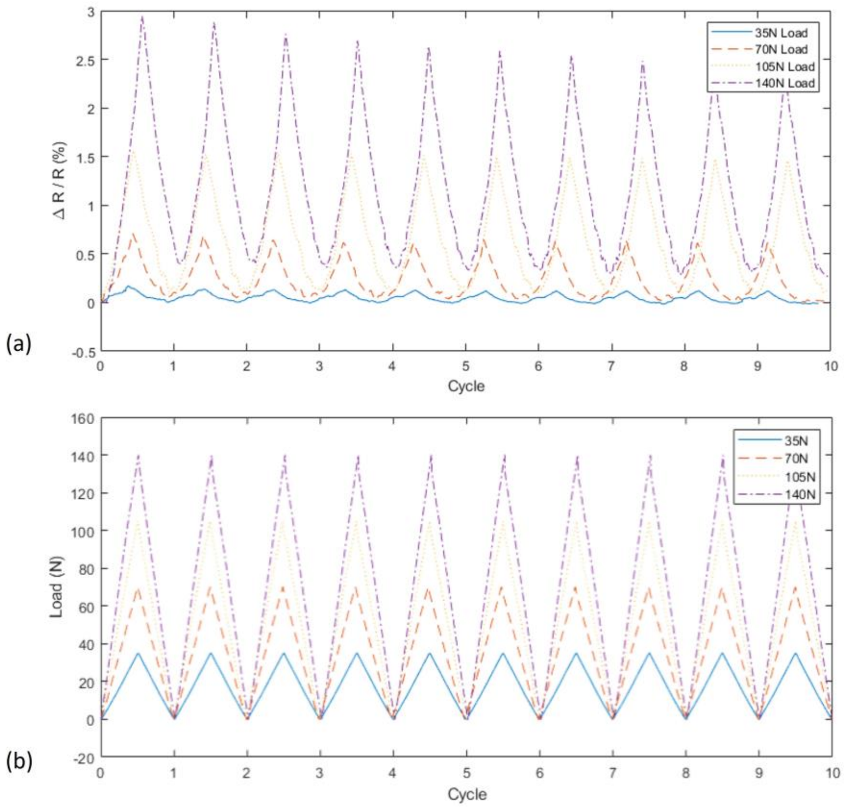

Figure 18. (a) Piezoresistive sensing signals under 3-point bending cyclic loads with four levels of maximum forces of 35 N, 70 N, 105 N, and 140 N; (b) applied cyclic loads

In the realm of strain sensing, the gauge factor (GF) stands as a paramount parameter to quantify a sensor's sensitivity. Essentially, the gauge factor is defined as the relative change in electrical resistance for a given strain, mathematically expressed as:

$$GF = (\Delta R/R)/\varepsilon_f$$

where ΔR represents the change in resistance, R is the initial resistance, and ε_f is the applied flexural strain calculated following the ASTM D790 standard in this thesis.

The GFs of the reported nanocomposite sensor are shown in Table 1. It is noted that the measured GFs were in the range of 25–103, while traditional metal strain gauges have the typical GF of 2–4 [31]. The significant increases in GF of 3D-printed nanocomposites are primarily due to the unique nanoscale interactions of MWCNTs, tunneling effects, and the reconfiguration of these nanofillers within the epoxy matrix in composites under the applied strains. Recognizing and understanding the GF is crucial, as it offers insights into the sensitivity and potential applications of the nanocomposite-based strain sensors in advanced technological domains.

Table 1. Calculated GF of embedded nanocomposite sensor in composite laminate

Applied Maximum Load (N)	35	70	105	140
GF	26	45	87	103

It has been reported that the performance of piezoresistive-based strain sensors can depend on external parameters, such as the applied load rate [32, 33]. In this thesis, the research team investigated how the applied three-point bending load rate can impact the sensitivity of the piezoresistive sensing signals. Three different levels of applied load rates, including 1 mm/min, 10 mm/min, and 20 mm/min, were applied up to 105 N maximum applied load. As shown in Figure 19, there were obvious differences in the piezoresistive signals. The peak of the piezoresistive signal variation ΔR/RΔR/R under the three load conditions was about 1%, 1.5%, and 3.5%. Since the GF of the piezoresistive sensors were linearly correlated to the piezoresistive signal variation ΔR/RΔR/R, the GFs of the same nanocomposites depended on the applied load rates. Therefore, the sensitivity and related GF were different at these three loading conditions. This experimental study revealed that the piezoresistive sensing capability of nanocomposite sensors exhibited a distinct dependence on the load rate. Specifically, at rapid load rates, the sensors tended to demonstrate higher sensitivity owing to the more pronounced reconfiguration and realignment of MWCNT nanofillers within the polymer matrix. This heightened sensitivity resulted in a more pronounced change in the electrical resistance of the sensor for a given amount of strain. Conversely, at slower load rates, the rearrangement of nanofillers was more gradual, potentially leading to a diminished change in electrical resistance and, consequently, reduced sensitivity. Understanding this relationship is crucial for optimizing sensor performance in real-time applications and tailoring sensor responses to specific mechanical stimuli.

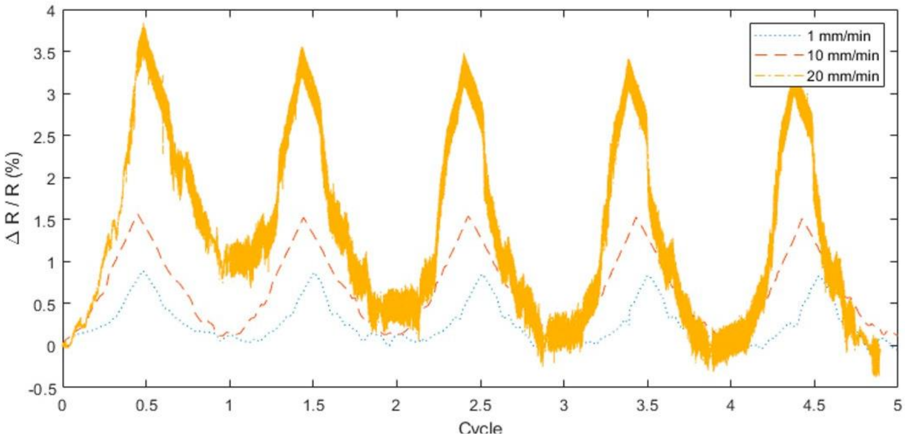

Figure 19. Piezoresistive sensor performance under various levels of applied load rates

To assess the durability and long-term performance of the embedded sensors, multiple cyclic tests were conducted, and the piezoresistive sensor signals were continuously monitored throughout the tests. Given that these embedded sensors are intended for structural health monitoring (SHM) and damage diagnostics, their lifespan must exceed the designed service life of the composites. Evaluating the performance of the sensors under a high number of cycles is crucial for ensuring their reliability [34, 35]. Highly dependable sensors can not only reduce operational and maintenance costs but also enhance the structural safety and integrity of composite systems.

Figure 20 below shows the sensor performance with 105 N load up to 100 cycles. Throughout this test, the peak-to-valley values of each piezoresistive signal cycle remained consistent. However, there was a slight reduction in the maximum and minimum electrical resistance, potentially due to the realignment of MWCNTs during the cyclic tests. The consistent peak-to-valley sensor signals indicated the highly repeatable and reliable load-sensing capabilities of the embedded sensors within composite laminates.

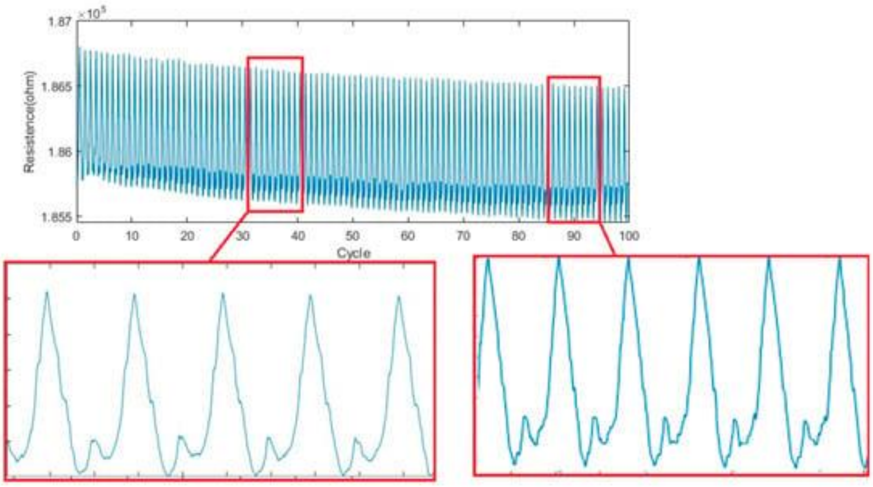

Figure 20. Piezoresistive sensor performance under three-point bending loads up to 100 cycles

The 1000-cycle cyclic tests were conducted to further investigate the long-term performance of the embedded nanocomposite sensors in composite laminates. The typical sensor performance is shown in Figure 21. It is noted that the peak-to-peak piezoresistive sensing signal also remained consistent throughout these long-term tests. However, the maximum and minimum electrical resistance dropped in the first 100 cycles, but the reduction rate was visibly slowed later. The consistent peak-to-valley electrical resistance proved a strong proof of the robustness of the embedded sensor in cyclic load tests. It is reasonable to conclude that piezoresistive sensing single can still be a reliable indicator of the material's loading conditions. Once the measured load overpasses the allowed load levels, these sensor signals can be potential representations of any damage in composites for SHM analysis.

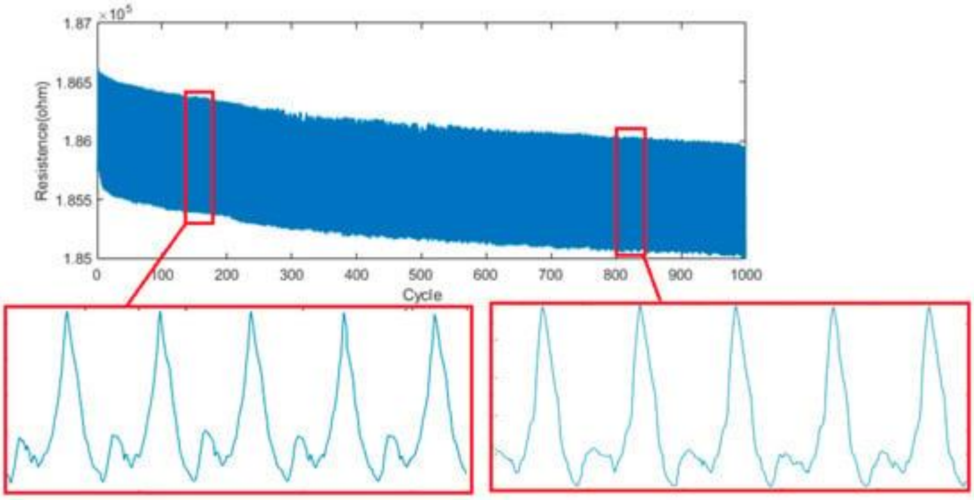

Figure 21. Piezoresistive sensor performance under three-point bending loads up to 1000 cycles

After undergoing long-term testing of 1000 cycles, the composite samples were further examined. Remarkably, even after these extensive tests, the samples could be tested for additional 100-cyclic tests without showing any significant signs of wear or degradation. The sensor performance was similar to the results reported in Figure 20. This resilience of the tested composite laminates with embedded sensors underscores the robust nature of the developed piezoresistive strain sensors, highlighting its potential for reliable service for SHM and damage diagnostics of structural composite applications and prolonged usage.

6. SEM Imaging and Failure Mode

The Thermo Fisher Quattro scanning electron microscope (SEM) was employed to examine the distribution of MWCNTs within the 3D-printed strain sensor. SEM images at various magnifications revealed the uniform dispersion of MWCNTs and the formation of a conductive network within the epoxy, contributing to the piezoresistive sensing capability. Additionally, the fractured areas of the composites following mechanical testing were analyzed to assess the failure modes and the quality of the manufactured composites. Given the low electrical conductivity of both epoxy and fiberglass fabrics, the composite surfaces were sputter-coated to prevent electric charge buildup during SEM imaging.

Uniform dispersion of MWCNTs was essential for establishing reliable piezoresistive sensing capabilities in the 3D-printed nanocomposite sensors. Due to their high surface area per unit volume, MWCNTs naturally tend to aggregate and agglomerate due to strong attractive interactions. However, shear mixing within the epoxy matrix successfully dispersed the MWCNTs, preventing agglomeration. Additionally, the shear forces generated during the DIW 3D printing process further dispersed the MWCNTs and aligned them in the printing direction, enhancing piezoresistive sensing performance. SEM imaging confirmed the absence of significant agglomeration, with a substantial portion of MWCNTs in contact, contributing to local contact resistance. Under applied strain, sliding between adjacent MWCNTs altered this contact resistance, enabling measurable sensing signals. In cases where MWCNTs were in close proximity but not physically touching, the tunneling effect became the dominant sensing mechanism. Changes in the distance between adjacent MWCNTs led to variations in tunneling resistance. The combined effects of contact resistance and tunneling resistance under applied strain produced measurable piezoresistive signals, facilitating strain measurement and potential damage diagnostics in the composite structures. Figures 22a and 22b show the cross-section of the nanocomposite sensor, and 22c/22d show the mating of resin and glass fiber.

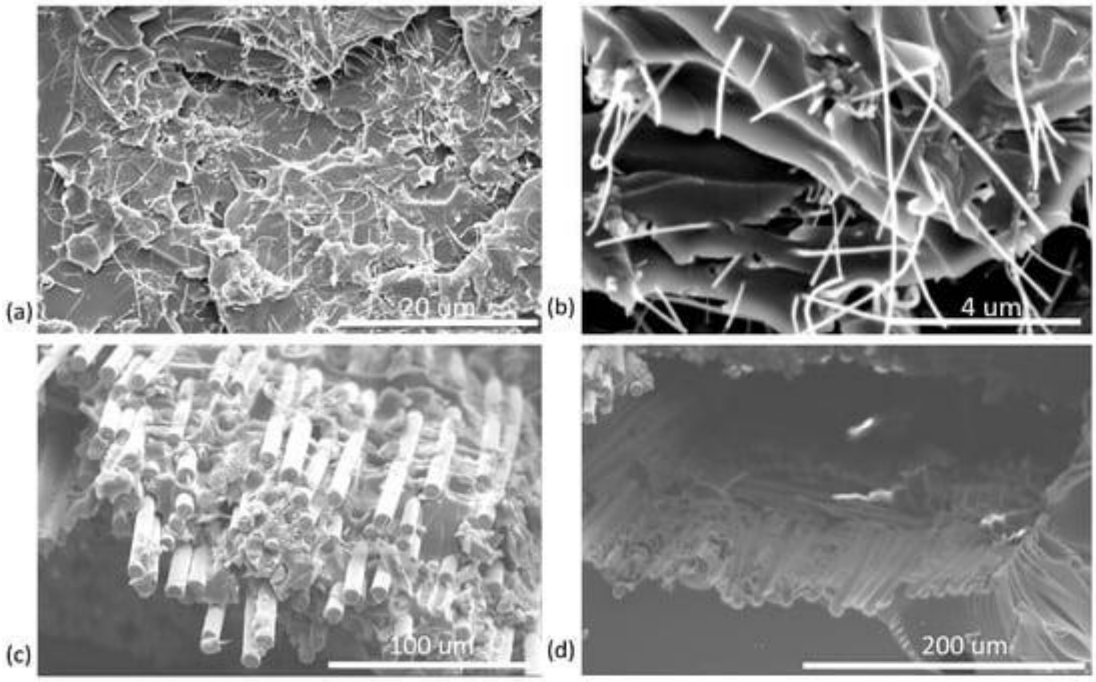

Figure 22. SEM images of embedded strain sensors and composites: (a,b) MWCNT distribution on the surface of 3D-printed nanocomposite sensors; (c) fiber pull-out on fractured surface of composite laminate; and (d) a socket left in the composite matrix after fiber

The composite manufacturing method used produced high-performance laminates. As shown in Figure 3c, fiber pull-out from the epoxy matrix occurred after fracture, indicating that this failure mode was the primary energy-absorbing mechanism responsible for increasing the toughness of the fiberglass composites. During crack formation, fibers were pulled from their sockets in the matrix, dissipating fracture energy over a larger area. This toughening mechanism helps prevent catastrophic failure in composite laminates. Figure 22d illustrates a typical socket left in the epoxy matrix following fiber pull-out. However, excessive fiber pull-out should be minimized to maintain high tensile strength in composites, which can be achieved by strengthening the fiber-matrix interface and improving bonding between the fibers and the matrix.

7. Conclusion and Future Work

This thesis showed the unique shape memory capacity of this nanocomposite, its versatility during printing, and sophisticated printing parameters. The developed nanocomposites showed both high 3D printability and an appropriate processing time window for material processing and curing. During the shape memory capacity testing, the material demonstrated robustness and flexibility when experiencing shape and temperature changes, showing its potential to achieve 4D printing with proper modification on the hardware. Printing parameters were discussed and recorded in detail, featuring layer height, travel speed, print pressure, ink viscosity, and others.

The development of 3D printed and embedded strain sensors for load monitoring in composite laminates for potential damage detection and SHM applications were also documented. The 3D-printed nanocomposite strain sensors were embedded within fiberglass fabrics reinforced composite laminates, and the piezoresistive sensor performance was tested under cyclic loads with the maximum loads of 35 N, 70 N, 105 N, and 140 N, and three load rates of 1 mm/min, 10 mm/min, and 20 mm/min. The experimental results demonstrated the highly repeatable piezoresistive sensing capability of the embedded sensors. The high sensor reliability was demonstrated in cyclic fatigue tests up to 1000 cycles. It is worth noting that the developed embedded sensors demonstrated exceptionally high sensitivity, achieving a maximum gauge factor exceeding 100. This study indicated the potential damage monitoring and load sensing capabilities using 3D printed and embedded nanocomposite strain sensors within structural composites for SHM applications.

There is much more work that can be done on the material preparation as well, which includes changing and testing new concentrations of curing agents and MWCNT, seeing how much change in mechanical and electrical properties it could bring. More printing parameters can be explored, such as different print patterns and layer heights, to tackle the over-extruding problem that occurs sometimes. The embedded sensor can also be improved by having different circuit thicknesses, patterns, and MWCNT concentrations. The test may not be limited to cyclic compression loading, but also vibration testing, as vibration monitoring [36] is heating up in today's mechanical engineering industry. Besides the reported self-sensing capability, additional nanocomposite functionalities, such as self-healing and self-powered sensors, can further increase the longevity and reliability of SHM systems. Integrating advanced data analytics and machine learning can also advance real-time damage detection and prediction, leading to the development of intelligent and adaptive composite structures. As the push towards more sustainable and intelligent infrastructure grows, these research directions are vital for the evolution of SHM applications.

Reference

1. Liu, Y. and S. Nayak, *Structural Health Monitoring: State of the Art and Perspectives*. JOM, 2012. **64**(7): p. 789-792.
2. Liu, Y., S. Mohanty, and A. Chattopadhyay, *Condition Based Structural Health Monitoring and Prognosis of Composite Structures under Uniaxial and Biaxial Loading*. Journal of Nondestructive Evaluation, 2010. **29**(3): p. 181-188.
3. Drobny, J.G., *3 - Additives*, in *Handbook of Thermoplastic Elastomers (Second Edition)*, J.G. Drobny, Editor. 2014, William Andrew Publishing: Oxford. p. 17-32.
4. Pham, H.Q. and M.J. Marks, *Epoxy Resins*, in *Ullmann's Encyclopedia of Industrial Chemistry*. 2005.
5. Miller-Stephenson. *Epon 862*. 2024 28 September 2024]; Available from: https://miller-stephenson.com/product/epon-862/.
6. Biron, M., *Chapter 4 - Detailed accounts of thermoset resins for moulding and composite matrices*, in *Thermosets and Composites*, M. Biron, Editor. 2004, Elsevier Science: Oxford. p. 183-327.
7. Montazeri, A., et al., *Mechanical properties of multi-walled carbon nanotube/epoxy composites*. Materials & Design, 2010. **31**(9): p. 4202-4208.
8. Davis, D.C., et al., *A strategy for improving mechanical properties of a fiber reinforced epoxy composite using functionalized carbon nanotubes*. Composites Science and Technology, 2011. **71**(8): p. 1089-1097.
9. Guadagno, L., et al., *Mechanical and barrier properties of epoxy resin filled with multi-walled carbon nanotubes*. Carbon, 2009. **47**(10): p. 2419-2430.
10. Zare, Y., K.Y. Rhee, and D. Hui, *Influences of nanoparticles aggregation/agglomeration on the interfacial/interphase and tensile properties of nanocomposites*. Composites Part B: Engineering, 2017. **122**: p. 41-46.
11. Zhao, D., et al. *3D Printed and Embedded Strain Sensors in Structural Composites for Loading Monitoring and Damage Diagnostics*. Journal of Composites Science, 2023. **7**, DOI: 10.3390/jcs7100437.
12. Haque, R.I., et al., *Self-powered triboelectric touch sensor made of 3D printed materials*. Nano Energy, 2018. **52**: p. 54-62.
13. Mondal, D. and T.L. Willett, *Mechanical properties of nanocomposite biomaterials improved by extrusion during direct ink writing*. Journal of the Mechanical Behavior of Biomedical Materials, 2020. **104**: p. 103653.
14. Abshirini, M., et al., *3D Printed Flexible Microscaled Porous Conductive Polymer Nanocomposites for Piezoresistive Sensing Applications*. Advanced Materials Technologies, 2022. **7**(9): p. 2101555.

15. Fadlurrahman, Z., et al., *Mechanical and chemical properties of matrix composite: Curing agent ratio, degassing process, and filler effect perspectives*. Journal of Engineering Research, 2023. **11**(4): p. 488-497.
16. Aleksendrić, D. and P. Carlone, *5 - Composite materials – modelling, prediction and optimization*, in *Soft Computing in the Design and Manufacturing of Composite Materials*, D. Aleksendrić and P. Carlone, Editors. 2015, Woodhead Publishing: Oxford. p. 61-289.
17. Kausar, A. and I. Ahmad, *Highpoints of carbon nanotube nanocomposite sensors—A review*. e-Prime - Advances in Electrical Engineering, Electronics and Energy, 2024. **7**: p. 100419.
18. Kushwaha, C.S., et al., *Advances in conducting polymer nanocomposite based chemical sensors: An overview*. Materials Science and Engineering: B, 2022. **284**: p. 115856.
19. Mishra, S. and B. Saha, *Graphene- polymer nanocomposite-based wearable strain sensors for physiological signal Monitoring: Recent progress and challenges*. Current Opinion in Solid State and Materials Science, 2024. **31**: p. 101174.
20. Reddy, Y.V.M., et al., *Strategies, advances, and challenges associated with the use of graphene-based nanocomposites for electrochemical biosensors*. Advances in Colloid and Interface Science, 2022. **304**: p. 102664.
21. Das, R., A.J. Pattanayak, and S.K. Swain, *7 - Polymer nanocomposites for sensor devices*, in *Polymer-based Nanocomposites for Energy and Environmental Applications*, M. Jawaid and M.M. Khan, Editors. 2018, Woodhead Publishing. p. 205-218.
22. Wu, Q., et al., *3D printing of a self-healing nanocomposite for stretchable sensors*. Journal of Materials Chemistry C, 2018. **6**(45): p. 12180-12186.
23. Yingtao, L., R. Abhishek, and C. Aditi. *Self-healing nanocomposite using shape memory polymer and carbon nanotubes*. in *Proc.SPIE*. 2013.
24. Abot, J.L., et al., *Delamination detection with carbon nanotube thread in self-sensing composite materials*. Composites Science and Technology, 2010. **70**(7): p. 1113-1119.
25. Zhou, L.-Y., J. Fu, and Y. He, *A Review of 3D Printing Technologies for Soft Polymer Materials*. Advanced Functional Materials, 2020. **30**(28): p. 2000187.
26. Xu, Y.-J., et al., *A novel and feasible approach for one-pack flame-retardant epoxy resin with long pot life and fast curing*. Chemical Engineering Journal, 2018. **337**: p. 30-39.
27. Nordson. *General Purpose Dispense Tips*. 2024 30 September 2024]; Available from: https://www.nordson.com/en/products/efd-products/general-purpose-dispense-tips.

28. Startsev, O.V., et al., *Comparison of Glass-Transition Temperatures for Epoxy Polymers Obtained by Methods of Thermal Analysis*. Mechanics of Composite Materials, 2020. **56**(2): p. 227-240.
29. Momeni, F., et al., *A review of 4D printing*. Materials & Design, 2017. **122**: p. 42-79.
30. Falahati, M., et al., *Smart polymers and nanocomposites for 3D and 4D printing*. Materials Today, 2020. **40**: p. 215-245.
31. Hoffmann, K., *An Introduction to Measurement Using Strain Gages*. 1989: Hottinger Baldwin.
32. Abshirini, M., et al., *3D Printing of Highly Stretchable Strain Sensors Based on Carbon Nanotube Nanocomposites*. Advanced Engineering Materials, 2018. **20**(10): p. 1800425.
33. Chowdhury, S.A., et al., *Highly Conductive Polydimethylsiloxane/Carbon Nanofiber Composites for Flexible Sensor Applications*. Advanced Materials Technologies, 2019. **4**(1): p. 1800398.
34. Loos, M.R., et al., *Enhanced fatigue life of carbon nanotube-reinforced epoxy composites*. Polymer Engineering & Science, 2012. **52**(9): p. 1882-1887.
35. Charara, M., et al., *Highly sensitive compression sensors using three-dimensional printed polydimethylsiloxane/carbon nanotube nanocomposites*. Journal of Intelligent Material Systems and Structures, 2019. **30**(8): p. 1216-1224.
36. Goyal, D. and B.S. Pabla, *The Vibration Monitoring Methods and Signal Processing Techniques for Structural Health Monitoring: A Review*. Archives of Computational Methods in Engineering, 2016. **23**(4): p. 585-594.